Environ Earth Sci (2011) 62:1461–1479
DOI 10.1007/s12665-010-0631-2

ORIGINAL ARTICLE

The use of multivariate statistical analysis of geochemical data for assessing the spatial distribution of soil contamination by potentially toxic elements in the Aljustrel mining area (Iberian Pyrite Belt, Portugal)

C. Candeias · E. Ferreira da Silva · A. R. Salgueiro · H. G. Pereira · A. P. Reis · C. Patinha · J. X. Matos · P. H. Ávila

Received: 6 October 2009 / Accepted: 15 June 2010 / Published online: 9 July 2010

Abstract Aljustrel mine is located in SW Portugal, in the western sector of the Iberian Pyrite Belt. The Aljustrel village was developed around the exploitations of massive polymetallic sulphides that occur in the area (4 orebodies mined, 2 in exploration phase). The pyrite ore was extensively exploited from 1850 to 1993, when production was discontinued. A mining restart occurred in 2008, only during a few months. The objectives of the study were to assess the levels of soil contamination, to determine associations between the different chemical elements and their spatial distribution, as well as to identify possible sources of contamination that can explain the spatial patterns of soil pollution in the area. Principal component analysis combined with spatial interpretation successfully grouped the elements according to their sources and provided evidence about their geogenic or anthropogenic origin. From this study, it is possible to conclude that soils around Algares/Feitais tailing deposits, Estéreis and Águas Claras mine dams and S. João mine show severe contamination. The highest concentrations of As (up to 3,936 mg kg^{-1}) and certain heavy metals (up to 321.7 mg kg^{-1} for Bi, 5,414 mg kg^{-1} for Cu, 20,000 mg kg^{-1} for Pb, 980.6 mg kg^{-1} for Sb, and 22 mg kg^{-1} Cd) were obtained near Algares area while the highest concentration of Cd (up to 61.6 mg kg^{-1}) and Zn (up to 20,000 mg kg^{-1}) were registered in samples collected in the S. João area. The highest pollution load index (>4.0) was recorded at the Algares area where the metal concentrations exceed typical soil background levels by as much as two orders of magnitude.

Keywords Soil · Multivariate data analysis · Geostatistics · Aljustrel mine · Environmental geochemistry

C. Candeias · E. Ferreira da Silva (✉) · A. R. Salgueiro · A. P. Reis · C. Patinha · P. H. Ávila
GeoBioTec-GeoBiosciences, Geotechnologies and Geoengineering Research Center, Departamento de Geociências, Universidade de Aveiro, Campus de Santiago, 3810-193 Aveiro, Portugal
e-mail: eafsilva@ua.pt

A. R. Salgueiro · H. G. Pereira
CERENA-Natural Resources and Environment Research Center, Instituto Superior Técnico, Av. Rovisco Pais, 1049-001 Lisbon, Portugal

J. X. Matos
LNEG-National Laboratory of Energy and Geology, Rua Frei Amador Arrais No. 39 r/c, Apartado 104, 7801-902 Beja, Portugal

P. H. Ávila
LNEG-National Laboratory of Energy and Geology, Lab. S. Mamede de Infesta, Rua da Amieira, Apartado 1089, 4466-901 S. Mamede de Infesta, Portugal

Introduction

The mining industry is probably the anthropogenic activity that produces the deepest impacts on the environment, since it is responsible for a complete transfiguration of the landscape and temporary elimination of the vegetation (Kelly 1988; Nriagu and Pacyna 1988; Nriagu 1989; Allan 1995; Salomons 1995; Starnes and Gasper 1995; Ripley et al. 1996; Alpers and Nordstrom 1999; Azcue 1999; Dold 2003). It also produces great amounts of solid, liquid and gaseous waste materials (Moore and Luoma 1990; UN/DTCD and DSE 1992; Alpers et al. 1994; Bigham 1994; Morin and Hutt 1997; Nordstrom and Alpers 1999; Kimball et al. 2000).

Mining gives rise to soil erosion and environmental contamination by generating waste during the extraction, beneficiation and processing of minerals. After closure, mines can still impact the environment by contaminating air, water, soil and wetland sediments from the scattered tailings, as well as pollution of groundwater by discharged leachate, unless the proper remediation is conducted. Heavy metal contamination of agricultural soils and crops surrounding the mining areas is a serious environmental problem in many countries (Bobos et al. 2006). The environmental impact on the mines surrounding is usually high and the related problems are mostly determined by the type of mineralization and by the procedures used during exploitation (Moore and Luoma 1990, Santos Oliveira et al. 2002). In short, the usually detected problems are (1) geotechnical and erosive instability through, for instance, large excavations and pits, (2) soils and waters contamination by mechanical dispersion of tailings, (3) wind pollution, (4) visual impact, urban and scenery disorder by the abandoned edifications and equipments.

Particularly within the mining industry, areas where polymetallic sulphides were extracted are important point and non-point sources of heavy metals. Small portions of metals occurring in mined ores, in general, are not totally recovered by mill and processing operations, and thus are left in tailings deposits. The piles of mine tailings (in general, fragmented and finely ground materials) left in the vicinity, constitute one of the greatest threats, since they present high concentration of heavy metals (As, Cd, Cu, Hg, Pb, Zn) and toxic chemicals. The presence of those piles implicates in the occurrence of "environmentally" sensitive locations, of unstable nature, in large number and often poor to non-existent maintenance. These materials when exposed to air and water, give rise to the oxidation of remaining sulphides, through chemical, electrochemical, and biological reactions, to form ferric hydroxides and sulphuric acid combined in acidic mine drainage (AMD) (Cohen and Gorman 1991; Merson 1992; Evangelou and Zhang 1995; Larocque and Rasmussen 1998; Soucek et al. 2000).

The fine soil fraction is also usually enriched in metals, due to the relative large surface area of fine particles for adsorption, to metal binding to iron and manganese oxides and to organic matter (Rasmussen 1998; Yukselen and Alpaslan 2001). Wind-blown dusts generated in those soils can be responsible for the atmospheric transport of trace metals (Rasmussen 1998). Therefore, soils are important sinks of heavy metals that could be inhaled, ingested, or absorbed, thereby entering the biosphere (Larocque and Rasmussen 1998). Heavy metals can persist in the soil over a long period of time and many of them are bioaccumulative or bio-magnified. This can result in long-term damage to flora and fauna and give rise to detrimental effects in humans, through introduction into the food chain and drinking water system (NRC 1974, NRC 1977; Bowie and Thornton 1984; Xu and Thornton 1985; Kabata-Pendias and Wlacek 1985, 2001).

Abandoned mines are one of the most serious environmental problems faced by many countries all over the world and Portugal is not an exception (Pereira et al. 2004). In order to characterize the number of old mines without owner or property rights the Portuguese Government has taken the responsibility to carry out an inventory and assessment of the abandoned mine sites. With this objective a comprehensive program has been developed in order to: (1) characterize and identify the generated impacts; (2) assess the symptoms of the risks inherent to former mining operations; and (3) promote measures that best fit the rehabilitation of the environmentally affected sites (Santos Oliveira et al. 2002). In the assessment, emphasis was given to several characteristics, such as: geology and mineralogy of the ore deposit, processes of ore extraction and processing, even size, composition and stability of the mine landfills (tailings), type and magnitude of chemical anomalies in soils, stream sediments and waters as well as actual mining safety, visual impact, degree of land use and archaeological (museum) relevance. About 80 derelict mine areas were studied in the Portuguese territory, as part of a restoration project developed by a partnership between the Portuguese Environmental Agency [Direcção Geral do Ambiente (DGA)], and the Portuguese Geological Survey [Instituto Geológico e Mineiro (IGM)], which mediates concessions for the exploration of geological resources. Presently, the Empresa de Desenvolvimento Mineiro public Company (the owner of the Portuguese mines rehabilitation program) is developing a rehabilitation program at mine activities' affected areas, before 1990 (Martins 2005; Nero 2005; Matos and Martins 2006). The Aljustrel mine in this assessment was classified as high risk and shows all sorts of problems occurring as consequence of the industrial activity closure and resulting lack of maintenance of the industrial-mining infrastructure.

The objectives of the present study were: (1) to evaluate the extent of pollution in soils impacted by mining activities and by erosion of the tailings; (2) to determine the associations between the different toxic elements and their spatial distribution, (3) to identify possible sources of contamination that can explain the spatial patterns of soil pollution in the area; and (4) evaluate the anthropogenic and lithogenic contribution.

Study area

Geographical location and physiographical aspects

Aljustrel is located in Beja district, approximately 175 km SE of Lisbon and 125 km N of Faro (Fig. 1a). The

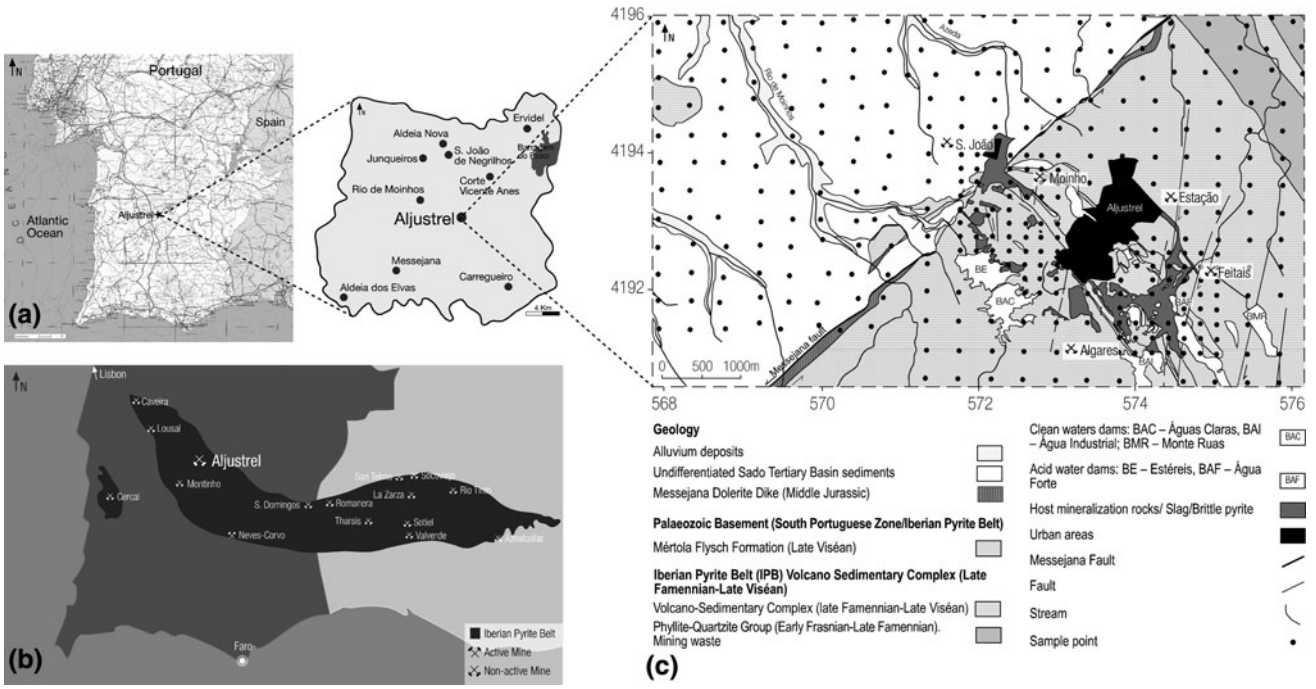

Fig. 1 **a** Location of the Aljustrel study region (adapted from http://google.brand.edgar-online.com/; http://www.agenda.pt/iframe.php?subcat=ALJUSTREL), **b** location of the Iberian Pyrite Belt region (adapted from Pacheco et al. 1998; Martins et al. 2003) and the Aljustrel study area; **c** geological setting and overlapping of the sampling grid, UTM coordinates in km (adapted from the Portuguese Geological Map 1/50,000, Schermerhorn et al. 1987)

Aljustrel complex mine is one of the great Iberian Pyrite Belt mining (IPB) sites (Fig. 1b), a world class volcanic hosted massive sulphides metalogenetic province (Barriga et al. 1997; Carvalho et al. 1999; Matos and Martins 2006; Oliveira et al. 2006; Relvas et al. 2006; Tornos 2006).

The Aljustrel area is located in the hydrographical Roxo River basin. The hydrographical network which drains the Aljustrel mine area is parallel type and, from west to east, the most important local streams are (1) Barranco do Farrôbo, (2) Água Azeda, (3) Água Forte. Like any other part of southern Portugal, Mediterranean climate predominates in the area. The area is much warmer and receives less rainfall than the national average. The temperature reaches a maximum of 40°C in summer (i.e., July and August) and a minimum of 5°C in winter (i.e., December). The mean annual rainfall in the area is estimated to be 550 mm, being the period from May to September very dry and wet from October to April (in average, 85% of the total annual rainfall occurs during this period). The highest amount of rainfall occurs in December, while July and August are the driest months. The catchment is dominated by rolling plains and arable lands. According to FAO soil classification (FAO 1999), soils of the study area were classified as Leptosols (occurring over a wide variety of parent rocks, mainly metasediments and acid volcanic–sedimentary materials), Luvisols (mainly associated to slates and greywackes) and Vertisols, Luvisols, Fluvisols and Cambisols associated to conglomerates and sandstones. Natural vegetation is mainly composed by *Quercus rotundifolia*, *Cistus ladanifer*, *Genista hirsute, C. salviifolius, C. crispus, C. monspeliensis* and *Lavandula luisieri*. In Aljustrel area, the *Quercus* forests have been replaced by eucalyptus plantations (*Eucalyptus camaldulensis*).

Geology and mineralization

According to Schermerhorn and Andrade (1971), Barriga (1990), Barriga and Fyfe (1988), Barriga et al. (1997), Relvas et al. (1990), Dawson et al. (2001), Carvalho et al. (1999) among others, the geology of Aljustrel region is characterized by a Palaeozoic basement of the South Portuguese Zone and by a modern sedimentary sequence of the Upper Sado Tertiary Basin. The active NE–SW Messejana fault defines the SE border of this basin, which is confined to the NW block of the fault (Fig. 1c).

The Messejana fault presents an Iberian dimension and a senestral strike–slip movement of 2.5 km. This fault separates the Sado Tertiary Basin (NW side of the fault) of the Palaeozoic (SE margin). Along this major structure a Jurassic Messejana dolerite (MD) is also observed (Schermerhorn et al. 1987).

According to several authors (Andrade and Schermerhorn 1971; Silva et al. 1997; Leitão 1998; Matos 2005; Oliveira

et al. 2006), the Aljustrel's Palaeozoic stratigraphic sequence is formed by the following main units:

Baixo Alentejo *Flysch* Group: Mértola Formation (Upper Visean)–shales and greywackes (flysch turbidites).

The IPB: Volcano–Sedimentary Complex (VSC) (Upper Famennian–Upper Visean) represented by the following units: Paraíso Fm.–siliceous shales, phyllites, tuffites, purple shales, jaspers and cherts; felsitic/mine metavolcanics and green metavolcanics sequences–sericitic felsic volcanics, felsites, felsophyres, volcanic breccias, massive sulphides, feldspar megacryst volcanics and lavas.

The IPB lower unit, the sedimentary Phyllite–Quartzite Group (Frasnian-Upper Famennian), is not recognized in the Aljustrel area. The VSC Aljustrel Anticlinorium is represented by a NW–SE lineament (4.5 km length and 1.5 km across).

In the Aljustrel mining site, six massive sulphide orebodies are recognized along a 6 km structure of VSC: Moinho, Feitais, Estação, Gavião, Algares and São João, the last two were mined since Roman times (Silva et al. 1997; Leitão 1998; Matos and Martins 2003, 2006). Moinho deposit was exploited by the Pirites Alentejanas Company (PA) for copper until 1993. The gossans and the supergene zones of the Algares and São João orebodies were exploited during roman era to 118-m deep in the first case (Domergue 1983). These massive sulphide orebodies have a mineralogy composed mainly by pyrite (FeS_2) (>70%), with minor quantities of sphalerite (ZnS), chalcopyrite ($CuFeS_2$), galena (PbS), arsenopyrite (FeAsS), tetrahedrite $(Cu,Fe)_{12}Sb_4S_{13}$), bornite (Cu_5FeS_4), pyrrhotite [Fe1-xS ($x = 0 - 0.17$)], cassiterite (SnO_2) and sulfosalts (Gaspar 1996).

Mining activity and environmental impact in the Aljustrel area

As a result of thousands of years of intense pyrite ores exploitation in Aljustrel, large areas are now occupied by several waste tailings such as Roman slag, pyrite ore (blocks and brittle massive pyrite ore—the most reactive ones) and VSC host rocks (Matos and Martins, 2006). Algares industrial area and S. João sector present the highest volumes of mine waste. The total amount of waste stored on the site exceeds 3 Mt. Those areas are affected by strong pluvial erosion, no vegetation and visible intense AMD.

The Algares and S. João outcropping massive sulphides orebodies were exploited during Roman time for copper and minor silver exploitation. The main objective of the Roman mining exploitation was the oxidation zones of the pyrite orebodies, characterized by extensive hematite supergene zones (Matos et al. 2003, Matos and Martins 2006). Since the nineteenth century and until the 1960s these orebodies were mined at surface (small open pits) and at underground galleries. The mine production was pyrite, roasted pyrite concentrates and copper obtained by cementation process at Pedras Brancas and Algares mine sectors (Martins et al. 2003). Between 1960s and the 1980s mining was dedicated to the Moinho and Feitais pyrite orebodies exploitation. The Moinho and Feitais ore deposits are formed by (Gaspar 1996): pyrite (FeS_2), sphalerite (ZnS), chalcopyrite ($FeCuS_2$) galena (PbS) and arsenopyrite (AsFeS). At Feitais also occurs tetrahedrite ($Cu_{12}Sb_4S_{13}$) and tennantite ($Cu_{12}As_4S_{13}$). The modern Aljustrel mine phase characterized by large volume of work (>1 Mt annual production of ore concentrates) occurs with the Cu concentrate production in 1990–1993 and with the Zn concentrate production in 2008. Minor and variable ore grades and problems with penalizing minor elements (e.g., Ta) were responsible by the short period of exploitation. The mining underground works are presently developed until ~400 m depth, focused again in the copper concentrate production (current ALMINA Mining Company project—Moinho and Feitais mining restart in 2010).

The small Mn–Fe mines located at the Aljustrel hills were exploited in the 19th century. The mine production was pyrolousite concentrates. Presently these abandoned mines are represented by small open pits and associated ore tailings, usually with less than 1 m thickness. Part of these small mines is used for illegal waste disposals. The environmental impact of these Mn–Fe exploitations is not quantified but is certainly locally significant.

Other mining wastes are present in Aljustrel, with less contaminant potential like host rocks, represented by felsic well cleaved and coherent volcanics, siliceous, purple and black shales, jaspers and cherts (Volcano–Sedimentary Complex host rocks). This pyrite host rock wastes were produced during the development of the pyrite underground mining works. Related with the cut and fill mining method important quarries were developed in areas were volcanic rocks outcrops. The main quarries located at the Malpique (Algares), Moinho and S. João mine sectors present significant geotechnical instability. Some of the mining infrastructures are unsafe and potentially dangerous, like open pits, quarries, galleries and mining shafts very exposed to local urban areas (Matos and Martins 2006).

Materials and methods

Sampling and chemical analysis

To investigate the impact caused by the dismantling and erosion of the tailings around the Aljustrel mine site, soil samples were collected in the area and analyzed. Soils were

sampled on two occasions: the first sampling campaign occurred during the summer of 2005 and encompassed soils from the VSC and Mértola Formation geological units (the Palaeozoic basement), and the second occurred in the summer of 2006 and encompassed soils from the Tertiary Basin. The studied area was monitored with a sampling network established on a 250 × 250 m grid in the centre of the contaminated area and 500 × 500 m in the remaining area (Fig. 1c). Each sampling point was georeferenced by Global Positioning System. A total of 356 soil samples were collected over an area of 44 km^2, corresponding to a sampling density of 8 samples km^2. At each sampling point, the surface of the soil was cleared of superficial debris, vegetation and the O-soil horizon. A composite sample consisting of three subsamples was collected (with a minimum distance between subsamples of 3 m) from the topsoil. According to the established grid the representativeness of the collected samples with the rock parent material is: 42.4% of samples is related with Tertiary Sado Basin Sediments (USTB); 36.5% with Baixo Alentejo Flysch group (MFF); 14.9% with Volcano–Sedimentary Complex (VSC); 4.5% with Phyllite–Quartzite Group; 1.7% with Messejana Dolerites (MD). After collection, the soil samples were dried in an oven at a temperature of 40°C, until a constant weight was attained, disaggregated and passed through a 177 μm aperture plastic sieve.

Superficial mine waste samples (upper 5 cm) were sampled by collecting 10-increment composites. About 1 kg of each sample was crushed with a jaw crusher and pulverized in a mechanical agate mill. The samples were reduced to 250 g by coning and quartering, followed by drying at 40°C. After homogenization aliquots of 30–50 g of each dried sample were powdered in a mechanical agate mill.

The fine grained fraction of soil and mine waste samples were submitted to multi-elemental analysis in an accredited Canadian laboratory (ACME Anal. ISO 9002 Accredited Lab-Canada). A 0.25 g split was leached in hot (95°C) aqua regia ($HCl–HNO_3–H_2O$) for 1 h and diluted with 10 mL of demineralized water. Total concentrations (detection limits between brackets) of As (0.5 mg kg^{-1}), Cd (0.1 mg kg^{-1}), Co (0.1 mg kg^{-1}), Cr (1 mg kg^{-1}), Cu (0.1 mg kg^{-1}), Ni (0.1 mg kg^{-1}), Pb (0.1 mg kg^{-1}) and Zn (1 mg kg^{-1}) were determined by Inductively Coupled Plasma-Emission Spectrometry (ICP-ES OPTIMA). The accuracy and analytical precision were determined using analyses of reference materials (USGS standard C3 and G-2) and duplicate samples in each analytical set.

Mineralogical studies

Minerals of the tailings samples were determined by powder XRD using a Phillips powder diffractometer, model PW3040/601, equipped with an automatic slit. A Cu-X-ray tube was operated at 40 kV and 30 mA. Data were collected from 2 to 70° 2θ with a step size of 1° and a counting interval of 0.6 s.

Data analysis

Statistical data analysis is a powerful tool in monitoring soil properties and assists in the interpretation of environmental data (Tuncer et al. 1993; Einax and Soldt 1999). In recent times, statistical methods have been applied widely to investigate heavy metals concentration, accumulation and distribution in soils, fact widely documented by a large number of reported studies which apply statistical methods to heavy metals in soils. Salman and Abu Rukah (1999), Lin et al. (2002) and Qishlaqi and Moore (2007) have used multivariate statistical methods to study the behaviour, distribution and interrelationship of heavy metals in soils. Therefore, statistical analysis of heavy metals in soil can offer an ideal means through which one can monitor not only the heavy metals accumulation in soil, but also the quality of the overall environment as it is reflected in soil.

Principal component analysis (*PCA*) this method aid in reducing the complexity of large-scale data sets and are currently broadly used in environmental impact studies (Perona et al. 1999) by elucidate relations among variables by identifying common underlying processes (Davis 1973, 1986; Webster and Oliver 1990; Wackernagel 1998). In the present study, a factorial analysis, PCA, was performed, using Statistica® (v. 6.0) software, allowing reducing the size of the space of the variables (Massart and Kaufman 1983). PCA main goal is to provide a small number of independent factors (principal components) which synthesize the associations between variables, being the referred factors (or PCs) orthogonal linear combinations of the variables. The first PC explains a major part of the total variance of the data set, and each successive PC explains a smaller part of the remaining variance. The different PCs are then related with common processes that affect the variables through expert knowledge of the problem in hand. The number of significant principal components for interpretation is selected on the basis of the Kaiser criterion with eigenvalue higher than 1 (Kaiser 1960) and a total of explained variance equal or higher than 70%.

Spatial estimation variography provides a description of the spatial pattern of a continuous attribute Z (or an indicator variable I_c), say a pollutant concentration of a chemical element (Reis et al. 2005) or the anomalous concentration of a metal orebodie with economic interest (Reis et al. 2004; Patinha et al. 2008). Given a data set for the variable Z at n locations x_i, ($Z(x_i)$, $i = 1, 2,\ldots,n$), the

sample variogram $\gamma^*_Z(h)$, the symbol * in this text will indicate estimates, measures the average dissimilarity between data separated by a vector h (Goovaerts 1999),

$$\gamma^*_Z(h) = \frac{1}{2N(h)} \sum_{i=1}^{N(h)} [Z(x_i) - Z(x_i + h)]^2 \quad (1)$$

where $N(h)$ is the number of data pairs at a lag of h. For I_c, the variogram is,

$$\gamma^*_{I_c}(h) = \frac{1}{2N(h)} \sum_{j=1}^{N(h)} [I_c(x_j) - I_c(x_j + h)]^2 \quad (2)$$

The variogram can be calculated for different directions of h, allowing to know how the variable $Z(x)$, or $I_c(x)$, varies in several directions of the space.

Ordinary kriging the main application of geostatistics to soil science has been the estimation and mapping of soil attributes in unsampled locations from nearby measured points in sampled areas. Kriging is a generic name for a family of spatial least-squares predictors. For the prediction of the variable Z at a location x_0, $\{Z(x_0)\}$, the estimator $Z^*(x_0)$ is defined as (Goovaerts 1999):

$$Z^*(x_0) = \sum_{i=1}^{n} \lambda_i Z(x_i) \quad (3)$$

where the λ_i are weights found by solving the system of equations,

$$\begin{cases} \sum_j^n \lambda_j \gamma(x_i, x_j) + \mu = \gamma(x_i, x), \quad i = 1, \ldots, n \\ \sum_j^n \lambda_j = 1 \end{cases} \quad (4)$$

with $\gamma(h)$ being the theoretical model for the variogram of the variable Z (fitted to the sample variograms) and μ being a Lagrange multiplier.

The software used to create variograms, to model variograms and perform spatial estimation based on Ordinary Kriging (including map generation) was Surfer® (v. 8.0).

Pollution load index (*PLI*) a quantitative approach of the multielement contamination was made based on the PLI according the methodology proposed by Tomlinson et al. (1980), by deriving the nth root of the n concentration factors ($CF_1 \times CF_2 \times CF_3 \times \cdots \times CF_n$ where n is the number of metals). The concentration factor (CF), defined as the ratio between each trace element in the soil sample and its background value (Galán et al. 2008). On account of the lognormal distribution of elements in geological materials (Salminen and Tarvainen 1997; Reimann et al. 2005), we assume the median (value at the 50th percentile of the background data) as soil geochemical baseline for each element, reflecting natural processes unaffected or diffusely affected by human activities.

Results and discussion

Statistical analysis, PCA analysis and spatial geochemical interpretation

The anomalous structures presents at the study area were described and resumed by the descriptive statistical analysis used. Table 1 resumes the summary statistics for the global dataset (soil and tailing samples), while Table 2 presents the summary statistics according to parent rock lithology. Table 1 show that the variables with higher distribution asymmetry are Cd > Zn > W > Cu > Bi > Mn > Pb > Mo > Co > Sb > As > Sn > Fe > P, all of them represent the elements of the common minerals of the Aljustrel massive sulphides orebodies. These results show contamination from brittle pyrite and ore host rocks tailings and mine infrastructures. According to the results of Table 2 is possible to see that soils collected in the Palaezoic Basement (VSC and also in Mértola flysch) are enriched in As, Bi, Cu, Fe, K, Mn, Mo, Rb, Sb, Sn Sr and Zn when compared with soils from Tertiary cover and from the Messejana dike. The median concentrations of As, Cu, Mo, Sb and Sn seem to distinguish the soils of VSC from the Mértola flysch, the first affected by hydrothermal

Table 1 Summary statistics for the global data set (soils and tailings concentrations in mg kg^{-1})

Variable	Mean	Median	Minimum	Maximum	Skewness
Al	68,101	68,600	13,000	137,300	0.07
As	99	18	6	3,936	7.26
Ba	375	374	4	1,147	0.71
Bi	5	0	0	322	8.74
Cd	0.6	0.2	0.1	61.6	16.55
Co	17	16	3	161	7.52
Cr	57	56	6	115	−0.05
Cu	135	39	10	5,414	9.04
Fe	40,389	36,400	10,500	341,300	6.18
K	15,226	15,100	3,100	32,400	0.37
Mn	1,184	811	19	27,522	8.67
Mo	1.6	0.8	0.2	41.8	7.89
Na	8,677	6,560	1,260	34,410	1.75
Ni	31	30	2	106	0.57
P	611	550	100	2,240	2.67
Pb	417	38	13	20,000	8.08
Rb	78	76	14	183	0.53
Sb	20.3	2.3	0.7	9,806	7.41
Sn	6	2	1	148	6.62
Sr	119	97	34	520	1.94
V	97	100	19	192	−0.07
W	2	1	0	39	9.37
Zn	233	88	22	20,000	13.92

Table 2 Statistical parameters of selected elements in soils according to parent rock lithology [Volcano–Sedimentary Complex (VSC), Phyllite–Quartzite group, Mértola Flysh Formation, Messejana Dolerites and Sado Tertiary Basin (USTB)]

	VSC ($n = 53$)				Phyllite–Quartzite Group ($n = 16$)				Mértola Fm. (Flysch) ($n = 130$)				Messejana Dolerite ($n = 6$)				Sado Tertiary Basin ($n = 151$)			
	Mean	Median	Min	Max	Mean	Median	Min	Max	Mean	Median	Min	Max	Mean	Median	Min	Max	Mean	Median	Min	Max
Al	66,466	67,900	13,000	105,100	98,088	99,500	62,500	137,300	76,097	76,100	14,300	125,900	68,967	77,800	39,900	91,600	58,528	57,900	17,700	90,900
As	384	63	13	3,936	20	18	11	38	95	22	6	2,578	24	18	12	49	17	15	6	105
Ba	393	412	6.0	1147	447	431	319	621	415	404	4	1,065	380	360	289	507	323	317	137	550
Bi	13	1.5	0.2	182	0.4	0.4	0.3	0.6	6.9	0.5	0.2	322	0.5	0.3	0.2	0.9	0.3	0.3	0.1	2.6
Cd	0.7	0.3	0.1	6.2	0.2	0.2	0.1	0.3	0.8	0.3	0.1	62	2.2	0.4	0.1	12	0.2	0.2	0.1	0.9
Co	16	17	3.0	63	22	21	16	33	17	15	5	161	17	17	10	30	16	15	6	29
Cr	41	37	5.8	81	84	87	55	115	61	63	6	114	70	76	58	83	56	53	15	99
Cu	324	180	22	1,640	54	50	29	117	156	53	11	2,774	89	39	21	357	32	29	10	186
Fe	58,004	40,600	13,800	341,300	42,150	42,200	24,900	57,300	43,583	38,800	18,500	23,8000	38,400	42,200	24,100	52,100	31,795	31,200	10,500	49,100
K	16,777	17,000	4,100	32,400	23,356	24,700	12,800	32,100	16,488	16,500	3,200	31,000	12,817	15,800	6,000	18,400	12,832	12,700	3,100	22,700
Mn	1,769	930	51	12,773	1,448	1,362	355	4,124	1,319	748	19	27,522	835	847	587	1,245	845	803	241	2,400
Mo	4.1	2.0	0.3	42	1.4	1.2	0.6	2.5	1.6	0.8	0.3	15	1.2	0.5	0.4	4.8	0.7	0.6	0.2	3.1
Na	6,818	6,070	1,290	18,120	6,263	6,010	2,870	9,830	12,810	10,970	1,360	34,410	7,453	5,750	1,950	22,300	6,109	5,130	1,260	31,490
Ni	26	25	2.0	58	45	44	27	65	32	32	2	106	35	42	21	51	31	29	8	57
P	701	610	210	2,240	658	630	470	950	635	570	100	2,220	625	660	380	890	549	520	200	1,380
Pb	1,445	144	20	20,000	32	31	17	52	541	56	16	20,000	109	54	32	425	34	28	13	191
Rb	98	98	24	170	121	113	72	163	83	82	14	183	62	79	31	84	64	66	16	113
Sb	64	9.3	1.1	811	1.7	1.7	0.7	3.4	26	3	1	981	3.3	1.7	1.3	9.1	2.2	2.1	0.8	8.1
Sn	14	6.3	2.2	116	3.0	3.0	2.4	4.1	7.2	2.7	1.0	148	2.1	2.0	1.3	3.0	2	2	1	6
Sr	134	105	40	520	121	97	72	297	149	138	47	300	97	94	68	171	88	78	34	427
V	78	75	19	192	129	131	86	166	105	105	20	185	119	119	82	161	93	92	32	175
W	3.6	2.3	0.8	28	0.9	0.8	0.5	1.3	1.8	1.2	0.3	39	1.0	1.2	0.6	1.7	1	1	0	2
Zn	314	167	67	2,233	71	75	36	103	310	108	49	20,000	1,237	158	43	6,852	72	64	22	569

All concentrations are given in mg kg^{-1}

Min minimum, *Max* maximum

alterations (Na-rich sericite and minor chlorite) while low median values in Ba are typical from soils related to Tertiary basin sediments. High values of Cd, Cr, Ni and P are typical from soils related to the Messejana dolerite. Such an asymmetry observed in the data is due to the presence of outliers, which can endanger the spatial continuity of the variogram function and produce poor results when using parametric techniques like ordinary kriging. However, in this study these difficulties are overcome as PCA produces new variables, the PCA components.

Principal component analysis reduces a set of observed variables into a smaller set of artificial variables called principal components (PC). This technique attempts to reveal the correlation structure of the variables allowing interpretation of geological processes affecting the soil geochemical data. PCs were extracted from the analysis of the matrix relating 356 soil samples × 23 variables.

Table 3 Factor loadings of each variable, variance, explained and cumulate variance of the principal components (PC)

	PC1	PC2	PC3	PC4	PC5
Al	**−0.5417**	**0.6571**	0.2565	−0.2082	−0.3106
As	**0.7754**	0.2294	0.2932	−0.0845	−0.0227
Ba	**−0.5328**	0.4550	0.0570	0.2794	−0.1732
Bi	**0.8466**	0.2467	0.2598	−0.1365	0.0534
Cd	0.3268	0.1993	**−0.8321**	−0.2114	−0.2388
Co	0.2666	**0.5113**	**−0.6460**	−0.2523	−0.0050
Cr	**−0.6238**	**0.5601**	0.0859	−0.3168	0.0949
Cu	**0.6223**	0.3049	−0.3334	−0.1594	−0.2016
Fe	**0.5888**	0.4995	0.1603	−0.0013	0.0271
K	−0.3472	**0.7825**	0.2754	−0.2491	0.0117
Mn	0.0202	0.3699	−0.3532	**0.7895**	−0.0367
Mo	0.4513	0.4281	0.0513	**0.5853**	0.0038
Na	−0.0831	−0.2793	0.2107	−0.1176	**−0.8206**
Ni	−0.4916	**0.6810**	−0.2757	0.0830	0.2142
P	−0.0765	0.2398	0.1726	0.2181	−0.0913
Pb	**0.8385**	0.2519	0.3059	−0.1274	0.0593
Rb	−0.2954	**0.6747**	0.2348	−0.1155	0.0656
Sb	**0.8914**	0.2665	0.2330	−0.1412	0.0523
Sn	**0.8617**	0.2704	0.2860	−0.0925	0.0417
Sr	0.0030	0.0449	0.2660	0.1018	**−0.8764**
V	**−0.5941**	**0.6165**	0.0719	−0.1504	0.0137
W	0.2404	0.3317	−0.0142	**0.8525**	−0.0801
Zn	0.3550	0.2271	**−0.8120**	−0.2240	−0.2529
Eigenvalue	6.64	4.45	2.85	2.35	1.82
Explained variance (%)	28.87	19.34	12.39	10.20	7.90
Cumulative variance (%)	28.87	48.21	60.60	70.80	78.70

Bold values represent factor loadings values higher than 0.5

Table 3 shows the factor loadings of principal components obtained by PCA statistical analysis using the element concentrations of the soil samples. According to the Kaiser criterion the number of significant principal components with eigenvalue higher than 1 was selected (Kaiser 1960; Davis 1986). Five principal components were considered in the factor analysis, accounting for 78.7% of the total variance of data.

The first component (PC1), explaining 28.87% of total variance, defines two groups of variables: Sb, Sn, Bi, Pb, As, Cu and Fe positively related, in opposition to Cr, V, Al and Ba variables, with high negative loadings. The second component (PC2), explaining 19.34% of total variance, reveals a group with high positive loading composed by K, Ni and Rb. Third component (PC3), which describes 12.39% of variance, has a high negative factor loading for the Cd, Zn and Co variables. Fourth component (PC4), accounting for 10.20% of total variance, has a high factor loading for W, Mn and Mo variables. PC5, explaining 7.90% of the total variance, has a high negative factor loading for Sr and Na. *P* variable is not explained by none of the five first principal components.

The overview of most representative variables projections allows distinguishing existing proximity and oppositions (Cardoso 1995). In Fig. 2a graphical projection of the PCA results discloses the position of the selected 23 variables coordinates, representing the correlation coefficients between the variables, in the different factorial plans. Five groups of variables can be identified in the four factorial plans.

In the first factorial plan (PC1/PC2, representing 48.21% of the global information of the data set), the selected variables could be separated into two groups. A first group (Group i—Fe, Cu, Pb, Sb, As, Bi and Sn) with positive loadings in PC1, reveals an association of elements strongly correlated between them with strong positive skewness. This group appears to be controlled by the mixed sulphide mineralization, as all elements presented in this factor are characteristic of the sulphide ore chemistry of Aljustrel representing the residual contamination within the study area. The antagonism between this group of variables and the metal concentration of V, Cr, Ba, Al, Ni, K and Rb (Group ii) could be clearly observed. This group shows small variability and represents an association of lithological elements driven by local geology.

In the second factorial plan (PC1/PC3, representing 41.26% of the global information of the data set), the association of Co, Cd and Zn (Group iii) variables is outlined. This association shows strong variability and skewness, as Group i, and represents an association of contaminant elements with strong mobility in acidic environments. Zinc-rich ores (common in the upper part of the Aljustrel pyrite lenses) usually present a good correlation with Cd values.

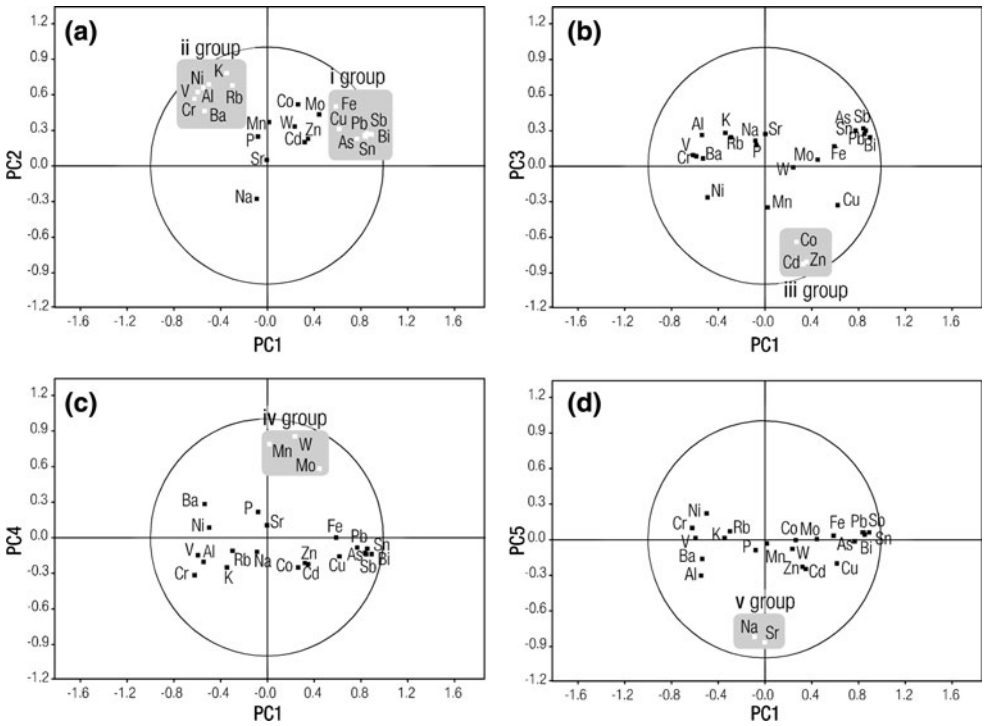

Fig. 2 Projection of the 23 variables on the four factorial plans **a** PC1/PC2, **b** PC1/PC3, **c** PC1/PC4, **d** PC1/PC5

The third factorial plan (PC1/PC4, representing 39.07% of total variance) is dominated by the association of W, Mn and Mo variables. This association indicates the presence of small manganese deposits related with jaspers and cherts horizons and siliceous and haematitic slates of the VSC forming the upper part of this Complex. These small nineteenth century old mines are located in the top of several hills of the Aljustrel region, related with the differential erosion of the jaspers and cherts. The Mn mineralization is composed, essentially, by Mn oxides, namely pyrolousite [MnO_2] and psilomelane [$Ba(Mn)^{2+}(Mn)_8^{4+}O_{16}(OH)_4$ or $(Ba,H_2O)_2Mn_5O_{10}$], where is also possible to find limonite [$2Fe_2O_3{\cdot}3H_2O$], hematite [Fe_2O_3] and baritine [$BaSO_4$]. The areas surrounding mineralizations are characterized by presenting high contents of Ba, Mn, Mo, Ni and W.

The fourth factorial plan (PC1/PC5, representing 36.77% of total variance) is characterized by the association Na and Sr, which is characteristic of shales and greywackes of the flysch Mértola Formation.

Once interpreted the PCA results, according to expert knowledge of geochemical/geological processes within the study area, is now possible to assess the spatial distribution of the factors.

The first step was to determine the spatial structure of the new variables, for that experimental variograms were constructed and modelled according to the parameters given in Table 4. All variograms presented nugget effect (C_0) and were modelled with spherical functions. Graphical variograms and model fitted can be observed in Figs. 3, 4, 5, 6, 7.

Table 4 Parameters of model function fitted to the experimental variograms of the five PCs retained

PCs	C_0	Structure				
		Model	Main Direction	C_1	a_1 (m)	Anisotropy Ratio
1	0.180	Spherical	E–W	0.1085	1,640	2.00
2	0.070	Spherical	Isotropic	0.1235	1,200	1.00
3	0.002	Spherical	N83°E	0.1120	1,500	1.50
4	0.005	Spherical	N52°W	0.0970	2,000	1.25
5	0.043	Spherical	Isotropic	0.0360	3,300	1.00

C_0 nugget variance, C_1 sill, a_1 range

PCs 1 and 3 are related with contamination while all the others are related with local geology, as seen previously. The amplitudes (a_1) achieved for PCs 1 and 2 are very similar as well as the respective variogram main direction, therefore revealing some similarities in contamination spatial pattern distribution.

PCs 1, 2 and 5 present a high nugget effect (62, 36 and 54% of total variance, respectively), in opposition to PCs 3 and 4 that present nugget effect not higher that 5% of total variance. Since PCs are a variable that reflects the general behaviour of a group of elements, the existence of micro-scale variability of the field under investigation tends to increase. This aspect is even more highlighted when working in a mining area, where distribution of some elements in soils is influenced by the proximity to pollution sources, particularly in this mining area where mine waste deposit content has varied though out centuries.

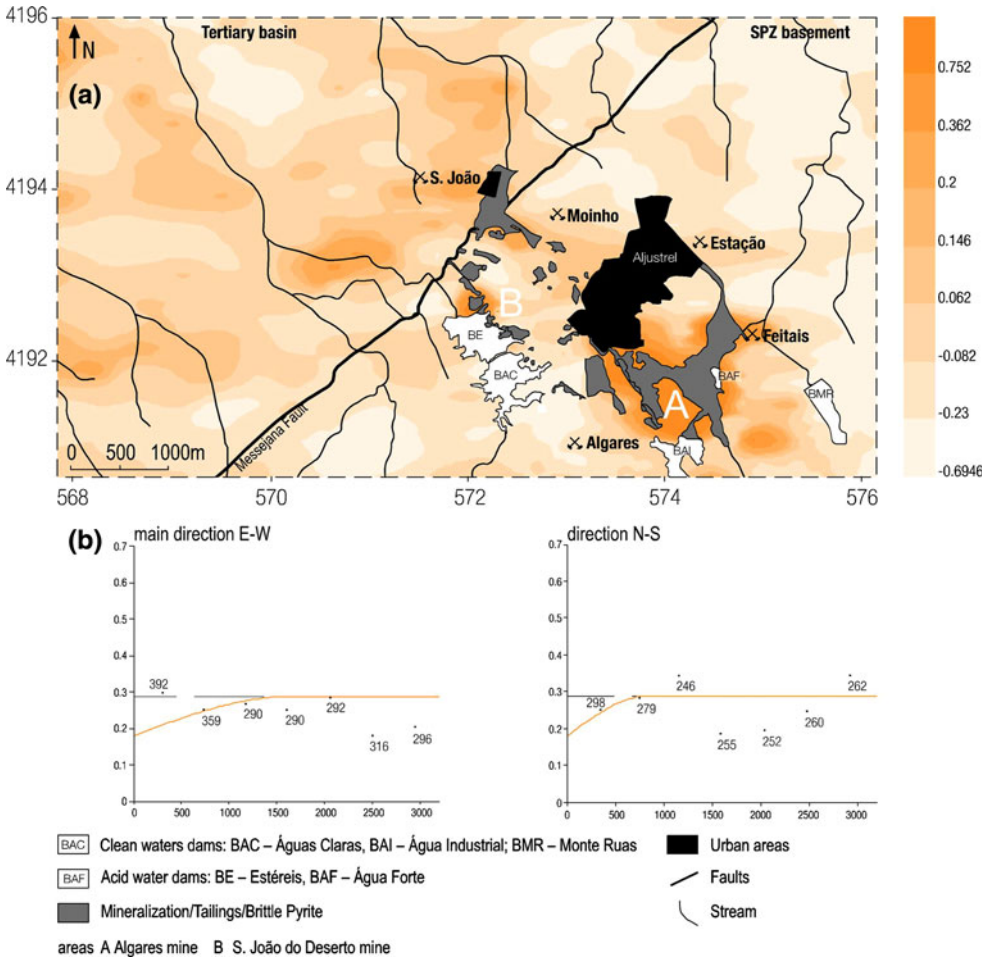

Fig. 3 Map of PC1 spatial distribution projected on the simplified map of the area (**a**) and respective variograms (**b**). High positive scores indicate geochemical anomaly for the element association: Fe, Cu, Pb, Sb, As, Bi and Sn well correlated with pyrite ore mine tailings (*A* Algares mine, *B* S. João mine)

In PCs 2 and 5 isotropic variograms were constructed, while the remaining PCs presented geometric anisotropy, as evidenced in Figs. 3, 5 and 6.

Estimation of the spatial distribution of each PC was then achieved by Ordinary Kriging and respective maps were produced (Figs. 3, 4, 5, 6, 7).

The estimated map of PC1 spatial distribution can be observed in Fig. 3. High positive values indicate geochemical anomalies, lie within the Algares/Feitais tailings (A) and the area of Estéreis Dam and Águas Claras Dam, near the S. João mine (B).

The spatial distribution of PC2 (Fig. 4), explained by K, Ni, Rb, Al, V, Ba and Cr variables, shows a strong connection to local geology, characterized by schist and greywacke of the flysch Mértola Formation. The greywackes turbidites are composed by quartz [SiO_2], feldspar (albite-oligoclase [$NaAlSi_3O_8$] and andesine [(Na,Ca)Al(Al,Si)-Si_2O_8]) and, rarely potassic feldspar [$KAlSi_3O_8$]. Biotite [$K(Mg,Fe)_3(Al,Fe)Si_3O_{10}(OH,F)_2$] is the most frequently mica. Grey hornblend [$Ca_2(Mg,Fe,Al)_5(Al,Si)_8O_{22}(OH)_2$] and piroxen [$(Na,Ca)(Fe,Mg)Si_2O_6$] also occur. As additional occurrences: titanite [$CaTiSiO_5$], apatite [$Ca_5(PO4)_3(OH,F,Cl)$], epidote [$Ca_2(Al,Fe)_3(SiO_4)_3(OH)$], ilmenite [$FeTiO_3$] and rarely rutile [$TiO_2$] and tourmaline [$(Na,Ca)(Mg,Li,Al,Fe^{2+},Fe^{3+})_3\ (Al,Mg,Cr)_6\ B_3Si_6\ (OH,O,F)_4$]. The shales are fundamentally composed by quartz [SiO_2] and sericite [$KAl_2(OH)_2(AlSi_3O_{10})$]. Commonly are present carbonates and minor sulphides in the shales and greywacke matrix. This composition supports the argument of a lithogenic control for this principal component.

Variables such as V, Cr, K and Rb define clearly the geological characteristics of VSC, represented essentially by felsic volcanic, black shales, green schists, haematitic purple shales and lenticular cherts and jasper. These rocks were formed in submarine environment. Regional hydrothermal alteration is responsible by the presence of alkalis (Na- and K-rich sericite). The porphyritic volcanics are quartz- and feldspar-rich whit a matrix sericitic to siliceous, locally chloritic. Near the massive sulphides the hydrothermal alteration system is characterized by proximal chlorite and silica-rich zones and distal sericite-rich zones (Barriga 1983, Relvas 1990; Relvas et al. 1990).

The spatial distribution of PC3 (Fig. 5) reveals a separation of soil samples related to the Sado Tertiary sediments, located at NW of the Messejana Fault, and the samples collected in the Palaezoic basement units (SC

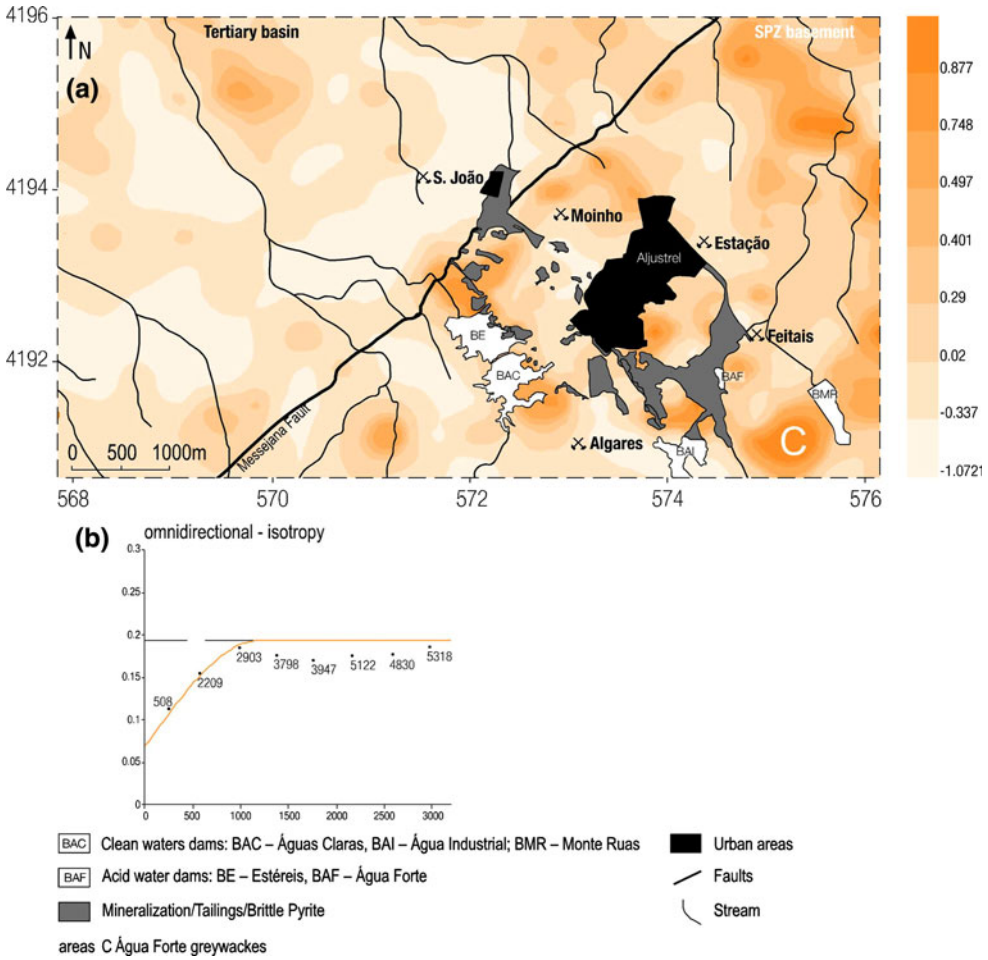

Fig. 4 Map of PC2 spatial distribution projected on the simplified map of the area (**a**) and respective variograms (**b**). High negative scores indicate geochemical anomaly for the element association: K, Ni, Rb, Al, V, Ba and Cr correlated with the presence of Tertiary sediments (*C* Água Forte greywackes)

volcanics and sediments and Mértola Formation turbidites). The Tertiary is Palaeogene and Miocene age and, composed by conglomerate, brechias, sandstones, claystones and carbonates (Schermerhorn et al. 1987). On the upper side of the sequence is possible to find a set of clays, sometimes atapulgite, marls with lime concretions, limes, sometimes with pebbles, and rosy or reddish argillaceous sandstone.

The spatial distribution PC4 indicates increased element concentrations at sample locations of high positive scores (Fig. 6), where is possible to observe a connection between the anomaly associated with small manganese deposits of the VSC and one of the oldest manganese mine (C), located near the Algares/Feitais area (A).

The separation between the geological units west of Mértola Formation, with sediments of Sado Tertiary Basin, by east of same fault, with volcanic rocks is patent on Fig. 7, which represents the spatial distribution of PC5.

PLI and environmental considerations

As noted from the PCA results, the soils close to the mining areas retain anomalously high concentrations of several potentially toxic elements rather than only one pollutant.

Considering the global data the As, Bi, Cd, Cu, Pb, Sb, Sn, and Zn are the most important variables to the PLI estimation (Table 5). PLI was calculated for each sample and estimated for the study area as shown on Fig. 8, where a constant behaviour (PLI < 2.0) over the Aljustrel area is to be highlighted.

The highest pollution load indices (PLI > 4.0) were recorded at the Algares mining area where the metal concentrations exceed typical soil background levels by as much as two orders of magnitude. By far, the largest Bi, Pb, Sb, As and Cu concentrations (outlier values) were recorded in soils near the Algares mine, while the most extreme value of Zn and Cd were obtained in soils near the S. João mine.

In the Algares area the concentration factor (CF) values are very elevated particularly for Bi (up to 3,217), Pb (up to 526.3), Sb (up to 426.4), As (up to 218.7) and Cu (up to 138.8) indicating severe soil pollution. According to the results this area contains very high levels of potentially toxic trace elements, although the total contents vary a lot

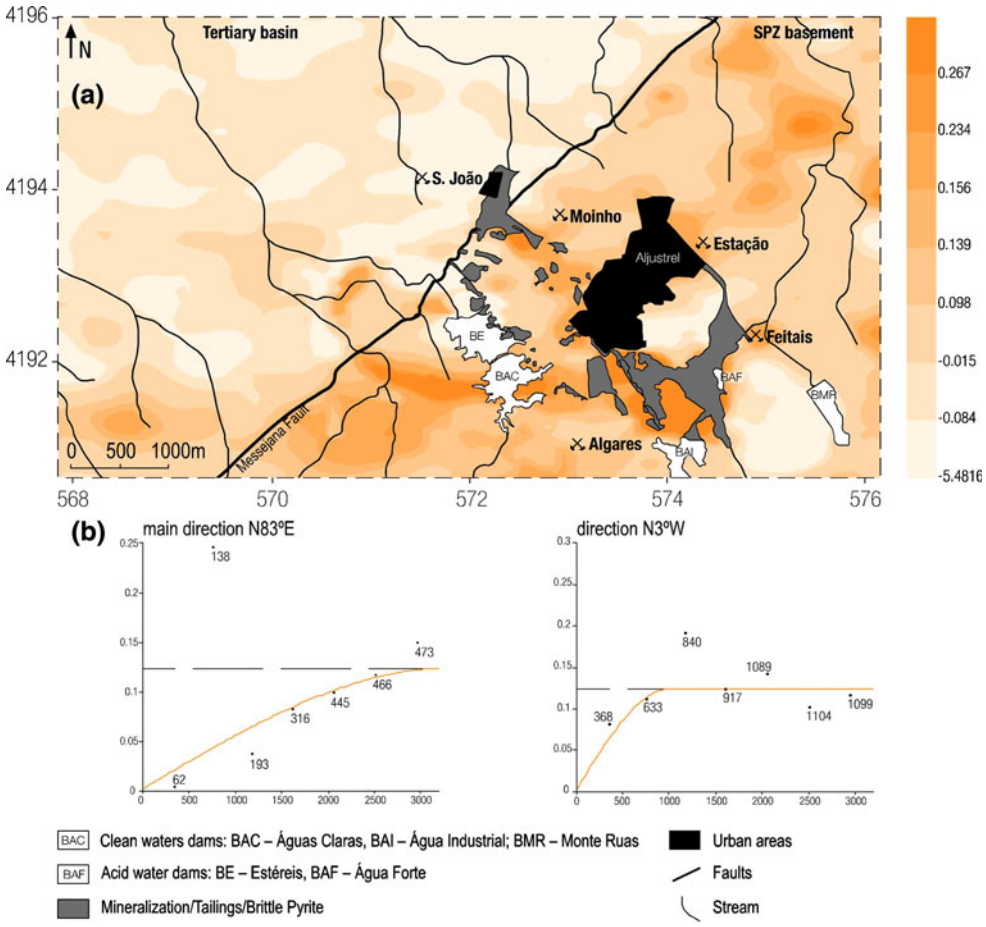

Fig. 5 Map of PC3 spatial distribution projected on the simplified map of the area (**a**) and respective variograms (**b**). High positive scores indicate geochemical anomaly for the element association: Co, Cd and Zn reflecting the Paleozoic basement units

depending on the location of the samples. Thus, the As concentration ranges widely from 120 to 3,936 mg kg^{-1}, being 541 mg kg^{-1} as the median value. The total abundances of Bi, Cu, Pb and Sb vary within more than two orders of magnitude, reaching concentrations as high as 321.7, 5,414, 20,000 and 980.6 mg kg^{-1}, respectively.

In the case of Co, Fe, and Mn, the CF fluctuates around the unit value, as expected for geogenic elements, since the average concentrations of such metals are within (or slightly above) the local geochemical baseline values (Table 5).

In the S. João mine area the PLI values ranges between 2.9 and 11.2. In this area the concentration factor (CF) values are also high particularly for Cd (up to 308.0), Zn (227.3) and Bi (165.0). According to the results this area contains very high levels of Bi (0.8–16.5 mg kg^{-1}), Cd (0.3–61.6 mg kg^{-1}) and Zn (205–20,000 mg kg^{-1}).

In the Algares (A) and São João (B) (Fig. 8) areas, the mine wastes consist of mixtures of weakly to strongly sulphidic rock and non-mineralized host rock materials (Matos and Martins 2006). In order to better explain the processes occurring in these areas results obtained in several representative samples from the different classes of mining wastes are presented in Table 6.

The geochemical study of mining waste samples revealed that pyrite ore present high concentrations of Fe, Cu, Pb, Zn, Ag, Sb, Hg, Sb, Co, Au, Cd while roasted pyrite ore shows high concentrations of Au, Pb, Ag, Fe, Sb, Bi, Sb, Cu, Zn, Mo. Roman slag presents interstitial pyrite and rare chalcopyrite with sparse distribution in the iron silicate matrix. The roman slag had high concentrations of Pb, Cu, Zn, Fe, As, Sb elements. Roman wastes are represented by in situ and reworked slags and are located in the upper stream sector of Água Forte stream (Matos 2005; Matos and Martins 2006). The mineralogical and petrographical study of ore waste samples allowed the identification of pyrite as the dominant sulphide, with interstitial chalcopyrite, sphalerite, galena, arsenopyrite and minor sulfossalts in the massive pyrite ore. The results show clearly that tailing deposits have high concentrations of Fe, Cu, Pb, Zn, Ag, Sb, Hg, Se, Co, Au and Cd. Roman tailings are enriched in Pb, Cu, Zn, Fe, As and Sb while iron oxides (roasted pyrite) are enriched in

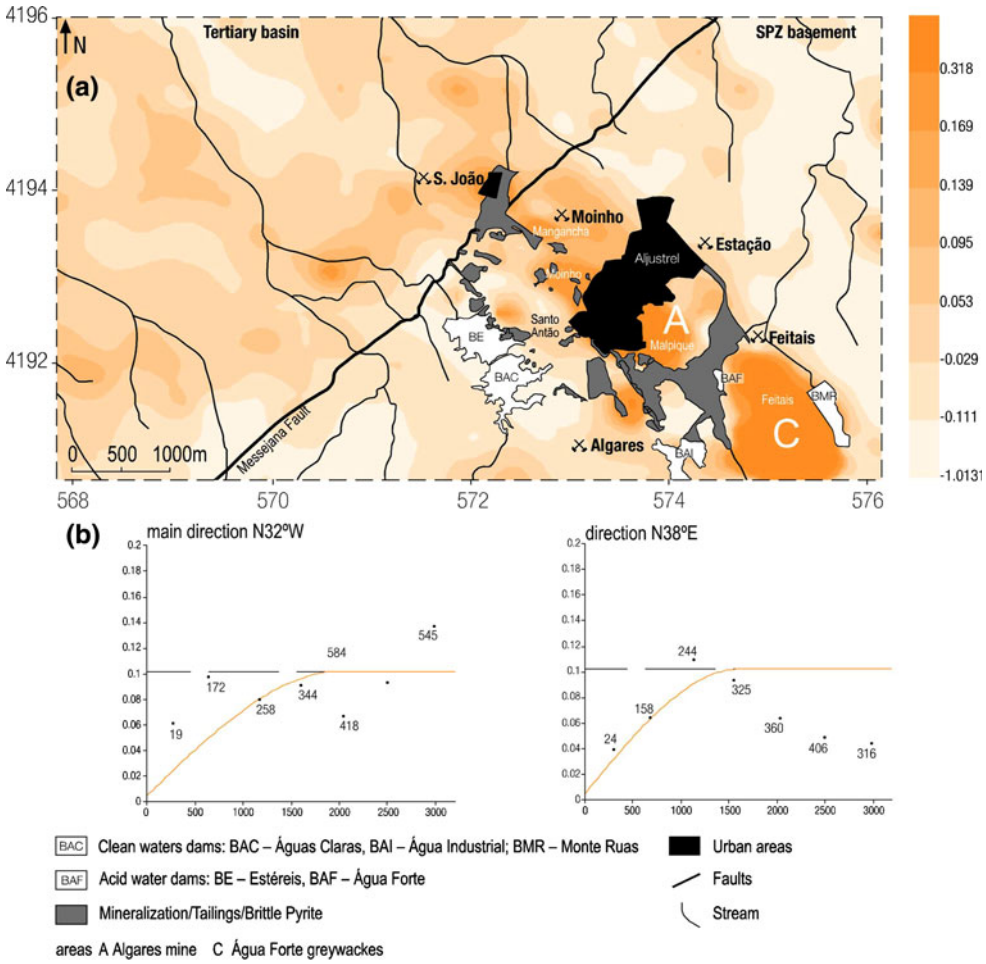

Fig. 6 Map of PC4 spatial distribution projected on the simplified map of the area (**a**) and respective variograms (**b**). High positive scores indicate geochemical anomaly for the element association: W, Mn and Mo. A good correlation is observed with the old Mn–Fe oxydes exploitations: Feitais, Malpique, Moinho, Mangancha e Santo Antão (*A* Algares mine, *C* Água Forte greywackes)

Au, Pb, Ag, Fe, Sb, Bi, Sb, Cu, Zn and Mo. These mine waste materials are undergoing reactions with air and rainwater, yielding white, green and yellow sulphate efflorescences and crusts, as well as leachates with very low pH. Sulphates include gypsum, halotrichite, melanterite type-phases, magnesiocopiapite, schwertmannite, and jarosite (Bobos et al. 2006). Many of these sulphates dissolve during rain events and subsequently precipitate on drying periods. Also goethite and hematite occur in the substrate material.

The presence of jarosite in topsoils and also in the mine waste materials creates additional contamination problems because jarosite act as temporary storage for acidity and may release this stored acidity upon hydrolysis and redissolution. Natrojarosite and natroalunite occurs also in veins in the Algares and São João gossans (Matos et al. 2003).

The exposure of pyrite-rich materials to weathering processes led to the dissolution of sulphide and gangue materials and consequently to the production of low pH, metal-rich waters and the associated chemical and physical mobilization of heavy metals and metalloids into the local drainage system. According to Luís et al. (2009) the AMD is responsible for an important impact in the local streams, namely: (1) Barranco do Farrôbo stream affected by the Sto. Antão new industrial area where the ore processing plant, the main acid water dam (Estéreis) and the Águas Claras clean water dam are located; (2) Água Azeda (AA) stream affected by the S. João mining sector (tailings and open pit) and by the São João urban area; (3) Água Forte (AF) main damaged area, stream affected by the Algares large brittle pyrite and slag tailings. Extremely high concentrations of trace elements in stream sediments and waters were registered, very different from background values and a decrease of diversity in diatom communities, elimination of sensitive taxa and shifts in taxonomic composition occur.

Also, Fernandes and Henriques (1989) have measured levels of Fe, Mn, Zn, Cu, and Pb in leaves and fruits of holm-oak (*Q. rotundifolia* Lain.) trees growing at the outskirts of the mining area. The trees showed pronounced stunting, reduced leaf size and extensive necrotic and

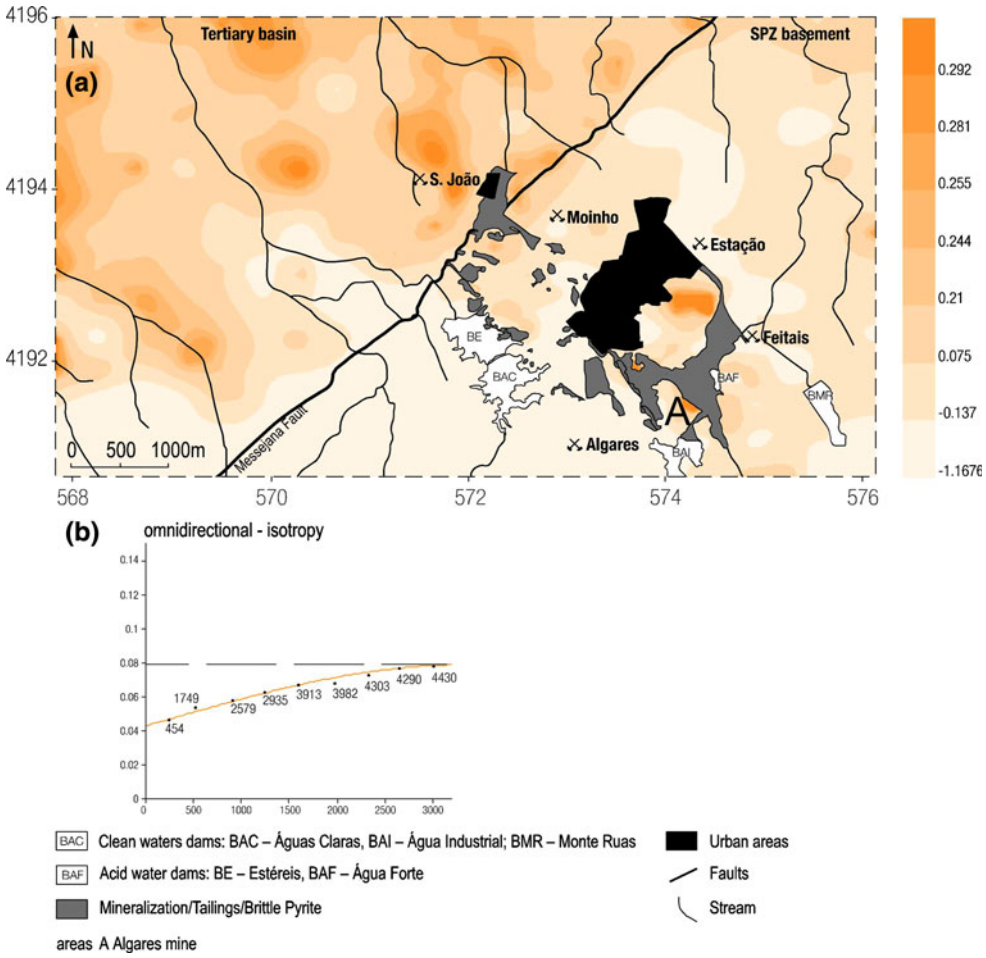

Fig. 7 Map of PC5 spatial distribution projected on the simplified map of the area (**a**) and respective variograms (**b**). High negative scores indicate geochemical anomaly for the element association: Na and Sr clearly associated with the Paleozoic basement flysch units (Mértola Fm.) geochemistry background (*A* Algares mine)

Table 5 Mean and range of concentration factors of the global data (soils and tailings), Algares area and S. João area and related Pollution Load Index (PLI) and the local geochemical baseline values (GBV)

	Global area ($n = 356$)			Algares area ($n = 24$)			S. João ($n = 9$)			GBV
	Mean	Min	Max	Mean	Min	Max	Mean	Min	Max	
CFAs	5.50	0.33	218.67	55.11	6.67	218.67	12.91	2.72	41.67	18
CFBi	47.42	1.00	3,217.00	610.83	15.00	3,217.00	53.11	8.00	165.00	0.1
CFCd	2.83	0.25	308.00	8.88	1.00	71.00	45.28	1.50	308.00	0.2
CFCo	1.05	0.19	10.06	1.19	0.25	5.06	2.29	0.44	10.06	16
CFCu	3.46	0.26	138.83	24.18	5.56	138.83	17.64	3.95	71.12	38
CFFe	1.11	0.29	9.38	2.64	0.90	9.38	1.59	0.98	3.46	36,400
CFMn	1.46	0.02	33.94	1.88	0.02	15.75	2.47	0.34	11.84	811
CFMo	1.96	0.25	52.25	8.44	1.50	52.25	3.79	1.00	13.63	0.8
CFPb	10.98	0.33	526.32	135.43	4.00	526.32	19.91	3.55	82.99	38
CFSb	8.83	0.30	426.35	102.45	4.61	426.35	18.64	3.96	64.26	2.3
CFSn	2.85	0.30	73.80	22.18	2.00	73.80	3.39	0.50	7.25	2.0
CFW	1.67	0.30	39.20	4.32	1.50	25.50	1.71	0.30	5.00	1.0
CFZn	2.64	0.25	227.27	9.67	1.18	92.06	38.87	2.33	227.27	88
PLI	2.03	0.43	26.67	10.53	4.27	26.67	5.52	2.91	11.21	–

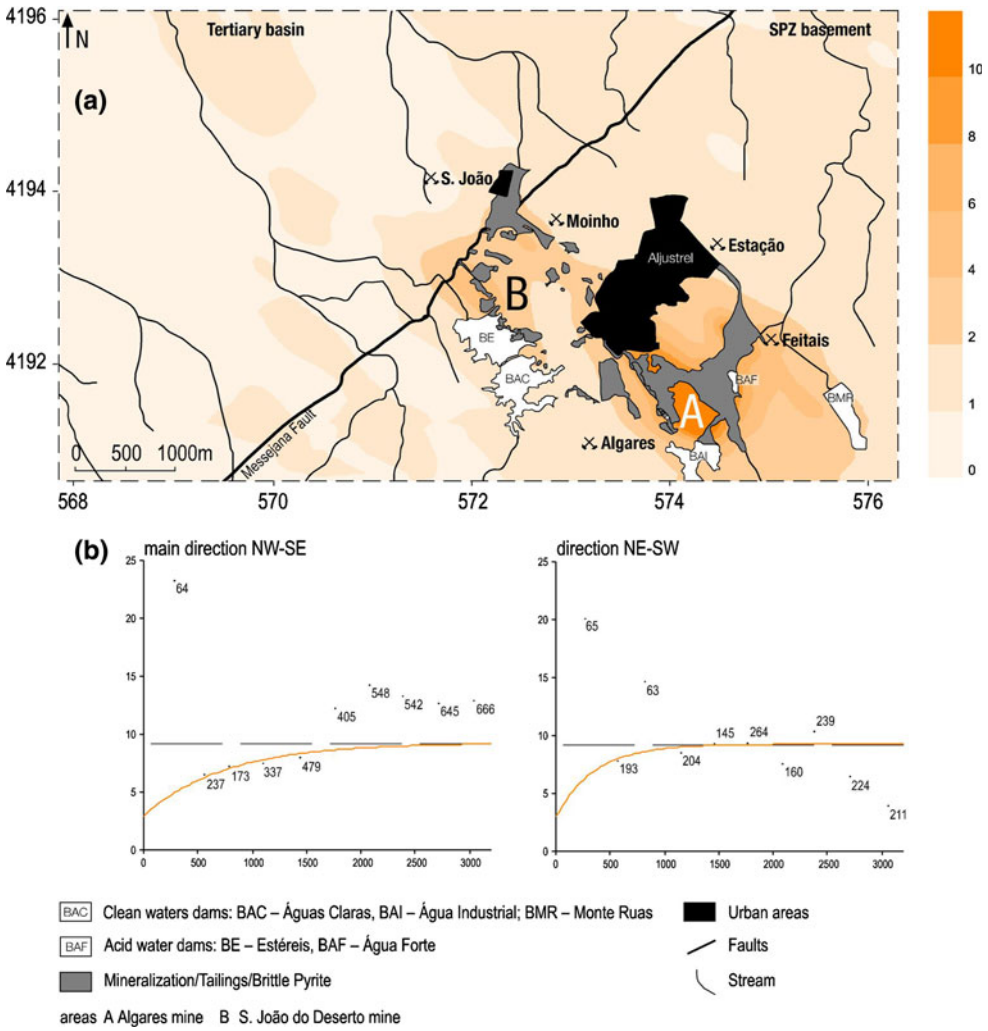

Fig. 8 Pollution load index (PLI) mapping (**a**) and respective variograms (**b**). PLI values were estimated on the basis of the concentration factors of As, Bi, Cd, Co,Cu, Fe, Mn, Mo, Pb, Sb, Sn, W and Zn (*A* Algares mine, *B* S. João mine)

chlorotic spotting. The leaves from trees growing in the area under study presented much higher concentrations of metals than the controls 50 times higher for Cu, 20 times for Pb and Zn, 10 times for Fe, and 2 times for Mn. The acorns from the contaminated areas were also metal polluted, particularly with Fe, Zn, and Cu, and this finding raises the threat of animal and human health hazards, since these fruits are commonly used for livestock feeding and are occasionally consumed directly by humans.

Conclusions

The Aljustrel mining area presents large areas affected by AMD related with dispersion of mining wastes: brittle pyrite ore, roman slags and sulphide mineralization host rocks. Soils near Algares and S. João areas have elevated As, Bi, Cd, Cu, Pb, Sb and Zn concentrations.

The combination of geochemical studies with multivariate data analysis and geostatistics revealed to be a powerful tool in the interpretation of processes in mining areas. PCA and geostatistical studies, especially ordinary kriging, gave an excellent support to estimate, with some accuracy, not only the associations of variables related to parent rocks but, mostly, the estimation of potential areas contaminated with heavy metals, in terms of associations of potential harmful elements instead of the common approach focused on individual element distribution.

Nevertheless, presently, there are few available data to assess the actual environmental hazard. Future research efforts should be addressed to enhance our understanding of the processes controlling metal speciation and bioavailability in the soils, and their influence on pathways leading to human and environmental exposures. This will be crucial in implementing soil remediation management strategies.

Table 6 Concentration of Mo, Cu, Pb, Zn, Ag, Co, Mn, Fe, As, Au, Cd, Sb, Bi, Hg and S in the selected tailing samples. Concentration values in mg kg^{-1} except for Fe and S (%)

Sample		Mo	Cu	Pb	Zn	Ag	Co	Mn	Fe	As	Au	Cd	Sb	Bi	Hg	S
EA-2	Algares coarse pyrite	15.8	2,392	2,708	7,572	>100	129	110	38.32	2,168	368	18.8	308.4	180.1	>100	>10
EA-3	Algares coarse pyrite	3.4	1,047	2,139	1,728	28.5	113	56	31.60	878	83	4.4	105.6	111.1	66.72	>10
EA-4	Algares coarse pyrite	5.2	854	7,437	1,057	25.3	95	52	21.47	1,258	201	3.5	98.6	111.7	58.71	>10
EA-5	Algares coarse pyrite	6.6	4,021	3,427	1,714	21.3	105	57	28.12	2,191	188	3.9	129.8	82.2	50.49	>10
EA-6	Algares coarse pyrite	3.8	800	2,898	646	16.2	94	35	26.85	722	147	2	107.9	89.6	44.2	>10
EA-11	Algares coarse pyrite	11.8	580	2,190	3,301	43.1	111	82	36.71	1,206	20	7.3	314.1	98.8	>100	>10
EA-15	Algares coarse pyrite	3.8	421	2,007	1,146	50.3	183	41	35.28	1,319	45	2.9	235.1	95.3	92.1	>10
EA-19	Algares brittled ore	14.5	>10,000	>10,000	>10,000	>100	60	51	27.34	1,971	436	24.6	>2,000	289.2	74.25	>10
EA-7	Host rock + ore (Algares)	9	577	2,906	103	7.3	5	20	22.99	2,335	62	0.2	119.5	64.7	12.45	4.02
EA-14	Host rock + ore (Algares)	3.8	1,407	4,154	295	17.5	9	124	11.54	1,158	107	0.5	1,23.6	41.1	26.19	2.88
EA-20	Host rock + ore (S. João)	15.9	747	2,008	509	3.5	78	1,915	5.69	457	50	1.2	58.2	8.5	0.34	0.07
EA-21	Host rock + ore (S. João)	2	237	1,866	233	7.1	3	119	7.86	524	128	0.4	54.5	34.2	23.81	2.56
EA-1	Algares cementation tank	8.5	472	3,114	318	9.4	2	41	34.89	4,139	116	0.7	186.2	86.4	15.3	4.53
EA-18	Algares cementation tank	0.2	4,515	148	>10,000	b.d.l.	98	5,821	4.48	177	1	47.4	4.7	0.2	0.11	8.87
EA-13	Algares roman slag	6.5	2,192	262	358	9.5	17	202	13.82	1,526	77	0.8	117.9	36.7	15.24	1.91
EA-8	Algares roman slag	3.7	5,536	3,133	645	5.9	31	354	15.1	483	26	0.9	52.4	14.2	1.3	0.86
EA-9	Algares roman slag	3.4	4,453	2,533	410	6.4	19	280	15.51	580	23	0.1	45.7	16.9	4.2	0.79
EA-10	Algares roman slag	4.5	3,311	2,069	269	3.6	16	749	7.77	381	18	0.2	28.6	12.4	3.46	0.36
EA-12	Algares roasted pyrite	31.2	282	>10,000	676	>100	33	109	25.14	9,033	2,594	3.3	1,787.4	681.2	>100	>10
EA-16	Cabeço do Homem Mn ore	8	65	79	58	b.d.l.	7	7,873	8.43	47	391	b.d.l.	1.6	0.7	0.19	b.d.l.
EA-17	Moinho Mn ore	14.3	9	89	700	b.d.l.	31	6,691	20.6	705	29	0.6	42.5	0.5	0.05	b.d.l.

b.d.l. below detection limit

Acknowledgments This study was carried out in the framework of the projects *e-Ecorisk—A regional Enterprise Network Decision Support System for Environmental Risk and Disaster Management of Large-Scale Industrial Spills (contract no. EV41-CT-2002-00068)* and *EVALUSE—Environmental Vulnerability of Aljustrel Mining Area in Terms of Land Use* supported by the European Union and FCT-Fundação para a Ciência e Tecnologia, respectively. The authors would like to thank the anonymous reviewers for their valuable comments which highly improved the manuscript.

References

Allan R (1995) Impact of mining activities on the terrestrial and aquatic environment with emphasis on mitigation and remedial measures. In: Salomons W, Forstner U, Mader P (eds) Heavy metals: problems and solutions. Springer, Berlin, pp 119–140

Alpers CN, Nordstrom DK 1999 Geochemical modeling of water-rock interactions in mining environments. In: Plumlee GS, Logsdon MJ (eds) The environmental geochemistry of mineral deposits. Part A: Processes, techniques and health issues, vol 6A. Reviews in economic geology, Littleton, Society of Economic Geologists, pp 289–323

Alpers CN, Blowes DW, Nordstrom DK, Jambor JL (1994) Secondary minerals and acid mine-water chemistry. In: Jambor JL, Blowes DW (eds) Short course handbook on environmental geochemistry of sulfide mine waste, vol 22. Mineralogical Association of Canada, Nepean, pp 247–270

Andrade F, Schermerhorn L (1971) Aljustrel e Gavião. Principais Jazigos Minerais do Sul de Portugal. Livro-Guia 4:32–59

Azcue J (ed) (1999) Environmental impacts of mining activities: emphasis on mitigation and remedial measures. Springer, Berlin

Barriga FS (1983) Hydrotermal metamorphism and ore genesis at Aljustrel, Portugal. PhD Thesis, University Western Ontario, London

Barriga FS (1990) Metallogenesis in the Iberian Pyrite Belt. In: Dallmeyer RD, Martinez García E (eds) Pre-Mesozoic geology of Iberia. Springer, Berlin, pp 369–379

Barriga FS, Fyfe WS (1988) Giant Pyritic base metal deposits: the example of Feitais (Aljustrel, Portugal). Chem Geol 69:331–343. doi:10.1016/0009-2541(88)90044-7

Barriga FS, Carvalho D, Ribeiro A (1997) Introduction to the Iberian Pyrite Belt, vol 27. Society of Economic Geologists, Guidebook Series, pp 1–20

Bigham JM (1994) Mineralogy of ochre deposits. In: Jambor JL, Blowes DW (eds) Short course handbook on environmental geochemistry of sulfide mine waste, vol 22. Mineralogical Association of Canada, Nepean, pp 103–131

Bobos I, Durães N, Noronha F (2006) Mineralogy and geochemistry of mill tailings impoundments from Algares (Aljustrel), Portugal: Implications for acid sulfate mine waters formation. J Geochem Explor 88:1–5. doi:10.1016/j.gexplo.2005.08.004

Bowie SHU, Thornton I (1984) Environmental geochemistry and health. Report the Royal Society's British national committee for problems of the environment. D. Reidel Publishing Company, Dordrecht

Cardoso JC (1995) Utilização da análise em componentes principais, variografia e krigagem factorial na identificação de anomalias geoquímicas, empregando sedimentos de linhas de água como meio amostral. PhD Thesis, Universidade de Aveiro

Carvalho D, Barriga FJAS, Munhá J (1999) Bimodal siliciclastic systems: the case of the Iberian Pyrite Belt. Rev Econ Geol 8:375–408

Cohen RRH, Gorman J (1991) Mining-related nonpoint-source pollution. Wat Environ Technol 3:55–59

Davis JC (1973) Statistics and data analysis in geology. Wiley, New York

Davis JC (1986) Statistics and data analysis in geology, 2nd edn. Wiley, New York

Dawson GL, Caessa P, Alverca R, Sousa JC (2001) Geology of the Aljustrel Mine area, southern Portugal. GEODE Workshop "Massive sulfide deposits in the Iberian Pyrite Belt: new advances and comparisons with equivalent systems", Aracena, Spain. Aljustrel, Eurozinc, Aljustrel Field Trip Guidebook

Dold B (2003) Secondary enrichment processes in sulfidic mine tailings: lessons for supergene ore formation. SGA News 16:10–15

Domergue C (1983) La mine antique d'Aljustrel (Portugal) et les tables de bronze de Vipasca. Conimbriga XXII:35

Einax JW, Soldt U (1999) Geostatistical and multivariate statistical method for the assessment of polluted soils; merits and limitations. Chemometr Intell Lab Syst 46:79–91. PII:S0169-7439-98.00152-X

Evangelou VPB, Zhang YL (1995) A review: pyrite oxidation mechanisms and acid mine drainage prevention. Crit Rev Env Sci Tec 25:141–199. doi:10.1080/10643389509388477

FAO (1999) World reference base for soil resources, 2nd edn. World Soil Resources. Report 103, Rome

Fernandes JC, Henriques FS (1989) Holm-oak (*Quercus rotundifolia* lam.) trees growing in a pyrites mining area at Aljustrel, Portugal. Water Air Soil Poll 48:409–415. doi:10.1007/BF00283338

Galán E, Fernández-Caliani JC, González I, Aparicio P, Romero A (2008) Influence of geological setting on geochemical baselines of trace elements in soils. Application to soils of Southwest Spain. J Geochem Explor 98:89–106. doi:10.1016/j.gexplo.2008.01.001

Gaspar OC (1996) Microscopia e petrologia de minérios aplicados à génese, exploração e mineralurgia dos sulfuretos maciços dos jazigos de Aljustrel e Neves-Corvo. Estudos, Notas e Trabalhos do IGM 38:3–195

Goovaerts P (1999) Using elevation to aid geostatistical mapping of rainfall erosivity. Catena 34:227–242. doi:10.1016/S0341-8162(98)00116-7

Kabata-Pendias A, Pendias H (2001) Trace elements in soils and plants. CRC Press, Boca Raton

Kabata-Pendias A, Wlacek K (1985) Excessive uptake of heavy metals by plants from contaminated soil. Soil Sci Ann 36:33

Kaiser HF (1960) The application of electronic computers to factor analysis. Educ Psychol Meas 20:141–151

Kelly M (1988) Mining and the freshwater environment. Elsevier Applied Science, London

Kimball BA, Bencala KE, Runkel RL (2000) Quantifying effects of metal loading from mine discharges. ICARD 2000: Proceedings from the fifth international conference on acid rock drainage, vol 2, pp 1381–1390

Larocque ACL, Rasmussen PE (1998) An overview of trace metals in the environment, from mobilization to remediation. Environ Geol 33:85–91. doi:10.1007/s002540050227

Leitão J (1998) Geologia dos depósitos de sulfuretos maciços de Aljustrel. Livro-Guia das excursões do V Congresso Nacional de Geologia, IGM, pp 91–100

Lin YP, Teng TP, Chang TK (2002) Multivariate analysis of soil heavy metal pollution and landscape pattern in Changhua County in Taiwan. Landsc Urban Plann 62:19–35. doi:10.1016/S0169-2046(02)00094-4

Luís AT, Teixeira P, Almeida SFP, Ector L, Matos JX, Ferreira da Silva EA (2009) Impact of acid mine drainage (AMD) on water quality, stream sediments and periphytic diatom communities in the surrounding streams of Aljustrel Mining Area (Portugal). Water Air Soil Poll 200:147–167. doi:10.1007/s11270-008-9900-z

Martins J (2005) Recuperação ambiental da área mineira de Aljustrel. III Encontro Comunidades Mineiras de Aljustrel, CM Aljustrel

Martins A, Alves H, Costa T (2003) 2000 anos de Mineração em Aljustrel; brochura da Exposição do Museu Municipal de Arqueologia de Aljustrel, Câmara Municipal de Aljustrel

Massart DL, Kaufman L (1983) The interpretation of analytical chemical data by the use of cluster analysis. Wiley, New York, p 65

Matos JX (2005) Carta geológica e mineira da Mina de Aljustrel esc. 1/5000, INETI

Matos JX, Martins LP (2003) Itinerários geo-ecoeducacionais como factor de desenvolvimento sustentado do turismo temático associado à Faixa Piritosa Ibérica. Abst. IV Cong. Int. Património Geológico y Minero, SEDPGYM, Utrillas, Espanha, pp 539–557

Matos JX, Martins LP (2006) Reabilitação ambiental de áreas mineiras do sector português da Faixa Piritosa Ibérica: estado da arte e perspectivas futuras. Boletín Geológico y Minero, Espanha, vol 117, no 2, pp 289–304

Matos JX, Barriga FJAS, Oliveira V (2003) Alunite veins versus supergene kaolinite/halloysite alteration in the Lagoa Salgada, Algares and São João (Aljustrel) and S. Domingos massive sulphide deposits, Iberian Pyrite Belt, Portugal. Rev. Ciências da Terra (UNL), Lisboa, pp B56–B59

Merson J (1992) Mining with microbes. New Sci 133:17–19

Moore JN, Luoma SN (1990) Hazardous wastes from large-scale metal extraction. Environ Sci Technol 24:1279–1285. doi:10.1021/es00079a001

Morin AK, Hutt NM (1997) Environmental geochemistry of minesite drainage. Practical theory and case studies. MDAG Publishing, Vancouver

National Research Council (NRC) (1974) Geochemistry of the environment: volume I, the relation of selected trace elements to health and disease. National Academy of Sciences, Washington

National Research Council (NRC) (1977) Geochemistry of the environment: volume II, the relation of other selected trace elements to health and disease. National Academy of Sciences, Washington

Nero G (2005) A problemática da recuperação ambiental das áreas mineiras degradadas a nível nacional. Abst. III Encontro Comunidades Mineiras de Aljustrel, CM Aljustrel

Nordstrom DK, Alpers CN (1999) Geochemistry of acid mine waste. In: Plumlee GS, Logsdon MJ (eds) Reviews in economic geology, the environmental geochemistry of ore deposits. Part A: Processes, techniques, and health issues, vol 6A, pp 133–160

Nriagu JO (1989) A global assessment of natural sources of atmospheric trace metals. Nature 338:47–49. doi:10.1038/338047a0

Nriagu JO, Pacyna JM (1988) Quantitative assessment of worldwide contamination of air, water and soils by trace metals. Nature 333:134–139. doi:10.1038/333134a0

Oliveira JT, Relvas JMRS, Pereira Z et al (2006) O Complexo Vulcano-Sedimentar da Faixa Piritosa: estratigrafia, vulcanismo, mineralizações associadas e evolução tectonoestratigráfica no contexto da Zona Sul Portugesa. In Dias R, Araújo A, Terrinha P, Kulberg JC (eds) Geologia de Portugal no Contexto da Ibéria, Universidade Évora, Portugal, VII Cong. Nac. Geologia, pp 207–244

Pacheco N, Carvalho P, Ferreira A (1998) Geologia da Mina de Neves Corco e do Vulcanismo do Anticlinório de Panóias—Castro Verde. V Congresso Nacional de Geologia. Livro Guia de Excursões

Patinha C, Correia E, Ferreira da Silva E, Simões A, Reis P, Morgado F, Cardoso Fonseca E (2008) Definition of geochemical patterns on the soil of Paul de Arzila using correspondence analysis. J Geochem Explor 98:34–42. doi:10.1016/j.gexplo.2007.10.001

Pereira R, Ribeiro R, Gonçalves F (2004) Plan for an integrated human and environmental risk assessment in the S. Domingos Mine Area (Portugal). Hum Ecol Risk Assess 10:543–578. doi:10.1080/10807030490452197

Perona E, Bonilla I, Mateo P (1999) Spatial and temporal changes in water quality in a Spanish river. Sci Total Environ 241:75–90. doi:10.1016/S0048-9697(99)00334-4

Qishlaqi A, Moore F (2007) Statistical analysis of accumulation and sources of heavy metals occurrence in agricultural soils of Khoshk River Banks, Shiraz, Iran. Am Eurasian J Agric Environ Sci 2:565–573

Rasmussen PE (1998) Long-range atmospheric transport of trace metals: the need for geosciences perspectives. Environ Geol 33:96–108. doi:10.1007/s002540050229

Reimann C, Filzmoser P, Garrett RG (2005) Background and threshold: critical comparison of methods of determination. Sci Total Environ 346:1–16. doi:10.1016/j.scitotenv.2004.11.023

Reis AP, Sousa AJ, Ferreira da Silva E, Patinha C, Cardoso Fonseca E (2004) Combining multiple correspondence analysis with factorial kriging analysis for geochemical mapping of the gold-silver deposit at Marrancos (Portugal). Appl Geochem 19:623–631. doi:10.1016/j.apgeochem.2003.09.003

Reis AP, Ferreira da Silva E, Matos J, Patinha C, Sousa AJ e Cardoso Fonseca E (2005) Combining GIS and stochastic simulation to define spatial patterns of variability for lead at the Lousal mine, Portugal. Land Degrad Dev 16:229–242. doi:10.1002/ldr.662

Relvas JMRS (1990) Estudo geológico e metalogenético da área de Gavião, Baixo Alentejo. Unpublished MSc thesis, University of Lisbon (Portugal)

Relvas JS, Massano C, Barriga F (1990) Ore zone hydrothermal alteration around the Gavião orebodies: implications for exploration in the Iberian Pyrite Belt; VIII Semana de Geoquímica, Lisboa

Relvas JMRS, Barriga FJAS, Ferreira A, Noiva PC, Pacheco N, Barriga G (2006) Hydrothermal alteration and mineralization in the Neves-Corvo volcanic-hosted massive sulfide deposit, Portugal: I. geology, mineralogy, and geochemistry. Econ Geol 101(4):753–790. doi:10.2113/gsecongeo.101.4.753

Ripley EA, Redman RE, Crowder AA (1996) Environmental effects of mining. St Lucie Press, Delray Beach

Salman SR, Abu Rukah YH (1999) Multivariate and principal component statistical analysis of contamination in urban and agricultural soils from North Jordan. Environ Geol 38:265–270. doi:10.1007/s002540050424

Salminen R, Tarvainen T (1997) The problem of defining geochemical baselines. A case study of selected elements and geological materials in Finland. J Geochem Explor 60:91–98. doi:10.1016/S0375-6742(97)00028-9

Salomons W (1995) Environmental impact of metals derived from mining activities: processes, predictions, prevention. J Geochem Explor 52:5–23. doi:10.1016/0375-6742(94)00039-E

Santos Oliveira JM, Farinha J, Matos JX, Ávila P, Rosa C, Canto Machado MJ, Daniel FS, Martins L, Machado Leite MR (2002) Diagnóstico Ambiental das Principais Áreas Mineiras Degradadas do País. Boletim de Minas 39:67–85

Schermerhorn L, Andrade R (1971) A Faixa Piritosa do Sul de Portugal; I Congresso Hispano-Americano de Geologia Económica; Livro-Guia da Excursão, n.° 4, Principais Jazigos Minerais do Sul de Portugal

Schermerhorn L, Zbyzewski G, Ferreira V (1987) Notícia Explicativa da Carta Geológica Portugal Fl. 42D, Sociedade Geológica de Portugal

Silva JB, Oliveira V, Matos J, Leitão JC (1997) Field Trip n°2, Aljustrel and Central Iberian Pyrite Belt. SEG Neves Corvo Field Conference. Guidebook series, vol 27, pp 73–124

Soucek DJ, Cherry DS, Currie RJ et al (2000) Laboratory to field validation in an integrative assessment of an acid mine drainage-impacted watershed. Environ Toxicol Chem 19:1036–1043. doi:10.1002/etc.5620190433

Starnes LB, Gasper DC (1995) Effects of surface mining on aquatic resources in North America. Fisheries 20:20–23

Tomlinson DL, Wilson JG, Harris CR, Jeffrey DW (1980) Problems in the assessments of heavy metal levels in estuaries and formation of a pollution index. Helgol Mar Res 33:566–575. doi:10.1007/BF02414780

Tornos F (2006) Environment of formation and styles of volcanogenic massive sulfides: the Iberian Pyrite Belt. Ore Geol Rev 28:259–307. doi:10.1016/j.oregeorev.2004.12.005

Tuncer GT, Tuncel SG, Tuncel G, Balkas TI (1993) Metal pollution in the Golden Horn, Turkey: contribution of natural and anthropogenic components since 1913. Water Sci Technol 28:50–64

UN/DTCD–UN, DSE, Department of Technical Co-operation for Development and German Foundation for International Development (1992) Mining and the environment. The Berlin Guidelines, Mining Journal Books Ltd, London

Wackernagel H (1998) Multivariate geostatistics: an introduction with applications, 2nd edn. Springer, Berlin

Webster R, Oliver MA (1990) Statistical methods in soil and land resource survey. Oxford University Press, Oxford

Xu J, Thornton I (1985) Arsenic in garden soils and vegetable crops in Cornwall, England: implications for human health. Environ Geochem Health 7:131–133. doi:10.1007/BF01786639

Yukselen MA, Alpaslan B (2001) Leaching of metals from soil contaminated by mining activities. J Hazard Mater B87:289–300. doi:10.1016/S0304-3894(01)00277-1